

Utah State University

DigitalCommons@USU

---

All Graduate Theses and Dissertations

Graduate Studies

---

5-2010

## Effects of Submergence in Montana Flumes

Ryan P. Willeitner  
*Utah State University*

Follow this and additional works at: <https://digitalcommons.usu.edu/etd>

 Part of the [Civil Engineering Commons](#)

---

### Recommended Citation

Willeitner, Ryan P., "Effects of Submergence in Montana Flumes" (2010). *All Graduate Theses and Dissertations*. 710.

<https://digitalcommons.usu.edu/etd/710>

This Thesis is brought to you for free and open access by the Graduate Studies at DigitalCommons@USU. It has been accepted for inclusion in All Graduate Theses and Dissertations by an authorized administrator of DigitalCommons@USU. For more information, please contact [digitalcommons@usu.edu](mailto:digitalcommons@usu.edu).



EFFECTS OF SUBMERGENCE IN MONTANA FLUMES

by

Ryan P. Willeitner

A thesis submitted in partial fulfillment  
of the requirements for the degree

of

MASTER OF SCIENCE

in

Civil and Environmental Engineering

Approved:

---

Steven L. Barfuss  
Major Professor

---

Michael C. Johnson  
Committee Member

---

Gary P. Merkley  
Committee Member

---

Byron R. Burnham  
Dean of Graduate Studies

UTAH STATE UNIVERSITY  
Logan, Utah

2010

## ABSTRACT

## Effects of Submergence in Montana Flumes

by

Ryan P. Willeitner, Master of Science

Utah State University, 2010

Major Professor: Steven L. Barfuss  
Department: Civil and Environmental Engineering

As part of a continued research project for the Utah Water Research Laboratory and the State of Utah, a study of flow measurement devices is being conducted throughout the state. Initially the project included only measurement devices associated with high-risk dams, but has since been broadened to any measurement structure of interest for water users in the state. The physical dimensions, relative elevations, and flow accuracy were documented for each included device.

After visiting sixteen sites, it was found that fourteen of the measuring devices had incorrect geometries. Of these fourteen, thirteen of them were originally Parshall flumes. A large percentage of Parshall flumes with geometry inaccuracies was also found from previous data collected for this project. One reoccurring issue was that the flumes had not been well maintained and had damage to the walls or floor. Some of these Parshall flumes did not have a diverging downstream section and are referred to as Montana flumes. In these cases, a standard Parshall rating curve was used to determine

flow where it did not apply. Some of the flumes that were tested operated regularly under submerged conditions, and no adjustments were made for submergence.

The objective of this research is to determine if Montana flumes (Parshall flumes without a diverging section) operate similarly to fully constructed Parshall flumes under both free-flow and submerged conditions. Laboratory tests were performed in the Utah Water Research Laboratory to determine corrections for submergence. *Flow 3D<sup>TM</sup>*, a computational fluid dynamics (CFD) software program, was also used to develop corrections for a submerged Montana flume. The laboratory results were compared to the computational fluid dynamics results. By using *Flow 3D<sup>TM</sup>*, a reliable numerical process was developed to determine the flow rate in a submerged Montana flume in an effort to expand the results to other sized flumes.

(54 pages)

## CONTENTS

	Page
ABSTRACT.....	ii
LIST OF TABLES.....	vi
LIST OF FIGURES.....	vii
LIST OF SYMBOLS AND ABBREVIATIONS.....	viii
CHAPTER	
I. INTRODUCTION.....	1
II. FLOW CORRECTION FOR A SUBMERGED MONTANA FLUME ....	6
ABSTRACT.....	6
INTRODUCTION.....	7
EXPERIMENTAL PROCEDURE.....	8
RESULTS AND ANALYSIS.....	11
Standard Parshall Rating Table.....	11
Parshall Submergence Correction.....	12
Transition Submergence.....	13
Testing Summary.....	14
Flow Correction.....	16
General Observations.....	16
APPLICATION.....	18
CONCLUSIONS.....	20
III. USING <i>FLOW 3D</i> <sup>™</sup> TO CORRECT FLOW RATES FOR A SUBMERGED MONTANA FLUME.....	21
ABSTRACT.....	21
INTRODUCTION.....	22
EXPERIMENTAL PROCEDURE.....	23
RESULTS AND ANALYSIS.....	27
Obtaining Results.....	27
Testing Summary.....	28
Laboratory Data Compared to Numerical Data.....	29
General Observations.....	30

		v
	APPLICATION .....	31
	CONCLUSIONS.....	34
IV.	SUMMARY AND CONCLUSIONS .....	35
V.	FUTURE RESEARCH.....	36
	REFERENCES .....	37
	APPENDICES .....	39
	Appendix A: Laboratory Photographs.....	40
	Appendix B: Images from <i>Flow 3D</i> <sup>TM</sup> .....	43

## LIST OF TABLES

Table	Page
1 Number of sites visited for this project .....	2
2 Transition submergence for laboratory data.....	14
3 Correction factors based on laboratory data.....	19
4 Percent deviation from laboratory data to numerical data.....	30
5 Correction factors for numerical data.....	33

## LIST OF FIGURES

Figure		Page
1	Range of submerged conditions. ....	8
2	Montana flume side view .....	10
3	Montana flume plan view .....	10
4	Downstream Ramp to increase submergence.....	11
5	Standard Parshall equations applied to laboratory data.....	12
6	High flow rates for 6-in. (15.2 cm) Montana flume. ....	15
7	Low flow rates for 6-in. (15.2 cm) Montana flume.....	15
8	Graphical correction for laboratory data .....	19
9	High flow rates using <i>Flow 3D</i> <sup>TM</sup> . ....	28
10	Low flow rates using <i>Flow 3D</i> <sup>TM</sup> . ....	29
11	Graphical correction for numerical data.....	32
12	Upstream subcritical conditions. ....	41
13	Hydraulic jump in the throat.....	41
14	Initial unstable flow.....	42
15	Secondary unstable flow.....	42
16	Initial water surface. ....	44
17	Flume meshing and geometry. ....	44
18	Refined mesh for stilling well. ....	45
19	Upstream geometry and mesh. ....	45
20	Downstream geometry and mesh. ....	46
21	Nested mesh sizing.....	46



## LIST OF SYMBOLS AND ABBREVIATIONS

List of Symbols

$A$	Length of the converging section in a Parshall flume (ft)
$a$	Coefficient used in the standard Parshall flow equation.
$b$	Exponent used in the standard Parshall flow equation.
$C_1$	Coefficient to calculate submergence
$C_2$	Coefficient to calculate submergence
$H_a$	Upstream head measurement (ft)
$H_b$	Downstream head measurement (ft)
$n_1$	Exponent to calculate submergence
$n_2$	Exponent to calculate submergence
$Q_{cor}$	Corrected flow rate (cfs)
$Q_s$	Submerged flow rate (cfs)
$Q$	Flow rate based on the standard Parshall rating curve (cfs)
St	Transitional submergence (%)
x	Horizontal distance to $H_b$ from the converging section (ft)
y	Vertical distance to $H_b$ from the converging section (ft)
$\alpha$	Submerged Montana flume correction factor

List of Abbreviations

CFD	Computational Fluid Dynamics
USBR	United States Bureau of Reclamation
UWRL	Utah Water Research Laboratory

## CHAPTER I

### INTRODUCTION

From 2007 to 2010 the Utah Water Research Laboratory performed a study to determine the accuracy of open-channel and closed conduit flow measurement devices throughout the state of Utah. By request from the state, 161 reservoirs were selected for the original study based on the criterion that they were high-risk dams. Of these reservoirs, 21 were visited which had various types of measuring devices. The flow was determined at five sites with electromagnetic flow meters, three using ultrasonic meters, and thirteen with Parshall flumes. Thirteen of the 21 calibrated structures were not measuring flow rate within the manufacturer's design criteria (Heiner 2009).

The state of Utah desired to further the study of other devices not associated with high-risk dams to determine the magnitude of inaccuracies at other flow measurement locations throughout the state. The Division of Water Rights assisted Heiner in visiting forty-nine additional flow measurement sites (Heiner 2009). The devices that were studied for that portion of the project include 48 Parshall flumes, eight Montana flumes, five ramp flumes, one Cutthroat flume, four weirs, one rated section, five ultrasonic meters, and five electromagnetic meters (see Table 1). The author joined this study near the end of 2009 to assist in inspection of the last eight measurement devices, and continued to inspect an additional eight structures that Heiner did not visit. Of the 16 structures the author visited, there were six Parshall flumes, eight Montana flumes, one ramp flume, and one sluice gate (see Table 1). Out of 78 measurement structures visited,

Table 1. Number of sites visited for this project

<b>Type of Measurement Device</b>	<b>Devices visited for the Project</b>	<b>Devices visited by the Author</b>
Parshall flume	48	6
Montana flume	8	8
Ramp Flume	5	1
Magnetic Meter	5	0
Ultrasonic Meter	5	0
Weirs	4	0
Rated Section	1	0
Cutthroat Flume	1	0
Sluice Gate	1	1
Total	78	16

two thirds of these structures did not meet design specifications for providing an accurate flow reading.

Due to the high percentage of measurement inaccuracies, finding the source of these errors was of great interest to the state. Many different conditions could justify these inaccuracies. The most common flaws noted throughout the project include, but are not limited to: stream line disruption, surface corrosion, staff gauge location, settlement, incorrect geometry, or submergence.

Streamlines through a flume are assumed to be parallel, and continuous (Parshall 1936). Many things can disrupt parallel streamlines such as sediment build-up on the bottom of the flume, vegetation growing in the flume, or debris hanging into the flume. Any of these conditions can disrupt the flow. If the flow past a stilling well port is not parallel to the wall on which the port is located, the static pressure will not represent a correct head. This error in upstream head,  $H_a$ , results in an inaccurate flow measurement.

Surface corrosion was occasionally found in structures tested by Heiner (2009).

Rust and worn concrete can change the dimensions of the flume where stringent dimensional accuracies need to be maintained (Parshall 1936).

Incorrect staff gauge locations were also commonly found at the various field sites. Additionally, none of the 61 flumes visited had staff gauges to measure the downstream head,  $H_b$ , when submergence did occur. Heiner (2009) used multiple stilling wells in a 2 ft Parshall flume to show a difference in head based on the location of the staff gauge. Stilling wells or staff gauge location for upstream measurement should be at a distance of  $2A/3$ . The distance  $A$  is the length of the vertical wall in the converging section (see Figure 3). Laboratory tests indicated that staff gauges placed near the throat of a Parshall flume, instead at the standard  $2A/3$  location, could result in up to 60% flow measurement error.

Settlement of a flume can be caused by numerous wet-dry, freeze-thaw, and heating-cooling cycles (Abt et al. 1995). Skogerboe et al. (1967) discouraged relying on a settled flume, but agreed that settling can occur after being in operation for a period of time. If lateral settling is minor, the discharge can still be accurately measured by finding an average depth of water on both sides of the flume at the  $2A/3$  location. Skogerboe indicates that settling near the exit section of the flume is common which can lead to erosion. This erosion can cause substantial damage to the flume, distorting accurate flow measurements. The discrepancy between the estimated discharge and the true discharge becomes greater as the amount of settlement increases. Genovez et al. (1993) also concluded that Parshall flumes are sensitive to the flume slope. For longitudinal slopes of  $\pm 5\%$ , errors in the rating curve were as large as 28% for free-flow conditions. For

lateral slopes of  $\pm 5\%$  the rating curve errors were 10% or less. Genovez suggests that those responsible for water measurement should consider initiating a program to check existing flume installations for settlement. A monitoring system would help maintain accurate flow measurements. In a study by Abt et al. (1994), lateral settlement had a substantial influence on a Parshall flume's rating under submerged conditions. When lateral settlement reached  $\pm 2\%$  the flume rating was in error 3%, 5%, and 11% for 70%, 80%, and 90% submergence. Abt et al. recommended that settlement should not exceed  $\pm 3\%$  for correct flow measurements even with adjustments.

Geometry is well defined and requires high accuracy to use a standard rating table for Parshall flumes. Throughout the state, many Parshall flumes had inaccurate geometries or missing sections. The original Parshall flume (Parshall 1936) specifies a radius wingwall to create a smooth transition into the flume. Nearly all the flumes in the field had an alternate 45-degree wingwall (USBR 2001). Parshall notes that at high flows a 45-degree wingwall causes a dip in the water surface elevation making staff gauges readings less reliable. Each dimension was specifically designated by Parshall (1936). According to the United States Bureau of Reclamation (USBR 2001) the tolerance on the throat width is  $\pm 1/64$  in., and the tolerances on other dimensions are  $\pm 1/32$  in. If these stringent design specifications are not followed, the flow readings could be in error. When an entire section is missing from a flume, the errors in geometry are well beyond a fraction of an in., which could drastically alter the flow readings.

Submergence occurs when changing conditions downstream of the throat alter the upstream head (Skogerboe et al. 1967). Along with free-flow conditions, Parshall (1936) also originally developed submergence curves to correct for downstream conditions that

impede free-flow. Robinson (1965) developed a graphical interpolation method to find corrections that were simpler than Parshall's correction method. If a flume is submerged beyond a certain point, specific for each size (USBR 2001), the standard Parshall rating curve cannot accurately predict the flow. Errors up to 60% result if no adjustments for submergence are made (USBR 2007). Further literature review regarding submergence is presented in Chapter II.

The literature indicates that data is available for correcting flow in a Parshall flume for staff gauge location, settlement, and submergence. Half of the structures visited by the author, however, were Montana flumes, which assume free-flow conditions and use Parshall (1936) calibrations. However, a quarter of the total structures visited were Montana flumes that operated occasionally or constantly submerged, and currently, there are no correction factors for Montana flumes in submerged conditions. Therefore, when a Montana flume operates under submerged conditions, the Parshall submergence corrections are normally assumed, and this "estimation" approach does not correct the flow accurately.

To determine these correction factors, a study was performed at the Utah Water Research Laboratory utilizing a 6-in. Montana flume. Chapter II discusses the laboratory experiments performed and the corrections that can be applied to a 6-in. Montana flume. Because the flumes found in the field were of various sizes, computational fluid dynamic software (*Flow 3D*<sup>TM</sup>) was calibrated to the data from the physical model so that the numerical model could also be extended to other sizes. The results from this exercise can be found in Chapter III.

## CHAPTER II

## FLOW CORRECTION FOR A SUBMERGED MONTANA FLUME

**ABSTRACT**

A Montana flume is a Parshall flume without a diverging downstream section. Tests were conducted on a Montana flume to determine the effects of submergence on flow readings. An acrylic 6-in. Montana flume was constructed to Parshall design dimensions with a 45-degree entrance wingwall and 90-degree exit wingwall configuration from the throat. The Montana flume was installed level in a 3 ft wide channel at the Utah Water Research Laboratory. A stilling well was placed on each side of the flume at the designated upstream and downstream locations,  $H_a$  and  $H_b$ , respectively. Staff gauges were also read to detect deviations from the stilling well readings. Twelve incremental flow rates were tested over a range of standard operation. For each flow rate, the head was measured as the submergence increased. Testing showed that a standard Parshall rating over-predicted the flow rates by 48%. Standard corrections were applied for submergence (Skogerboe 1967) and this approach under-predicted the flow rate by as much as 16%. Both of these methods established for determining flow rate are not within the designed 3-5% accuracy (Parshall 1936). This study developed new correction factors and their application is demonstrated for submerged Montana flumes.

---

<sup>1</sup> Coauthored by Ryan Willeitner and Steven L. Barfuss, P.E.

## INTRODUCTION

A design parameter made for Montana flumes is that they operate under free-flow conditions (USBR 2001). In this case, the same rating table used for Parshall flumes can be applied for Montana flumes because critical depth occurs in the throat. Unfortunately, half of the Montana flumes tested in the State of Utah (Heiner 2009) study were operating under submerged conditions, which alter the rating curve. The Water Measurement Manual (USBR 2001) makes the following comment on Montana flumes under submergence (*emphasis added*):

Care must be taken to construct Parshall flumes according to the structural dimensions given. This factor becomes more important as size gets smaller. The portion of the flume downstream from the end of the converging section need not be constructed if the flume has been set for free-flow where it is not expected to operate above submergence limit. This truncated version of the Parshall flume is sometimes referred to as the Montana flume. *Submergence corrections or discharge cannot be determined for Montana flumes or other modified Parshall flumes because they do not include the part of the full Parshall flume where the submergence head,  $h_b$ , was measured during calibration.* (p. 8-24)

The last statement is inaccurate because the downstream head,  $H_b$ , is in the throat of the flume, and the Montana flume incorporates this location (Figures 2 and 3). Due to the existence of several devices under this condition, research was performed to better understand submergence and to develop accurate flow rate correction coefficients for submerged conditions in Montana flumes.

According to Skogerboe et al. (1967), free-flow and submerged flow are the two most significant flow regimes or flow conditions in a Parshall flume. The difference is the occurrence of critical depth near the throat of the flume. Upstream of the throat, flow conditions are subcritical, and near the throat the flow regime may be supercritical. Experimentation does not indicate a unique submergence at which the change from



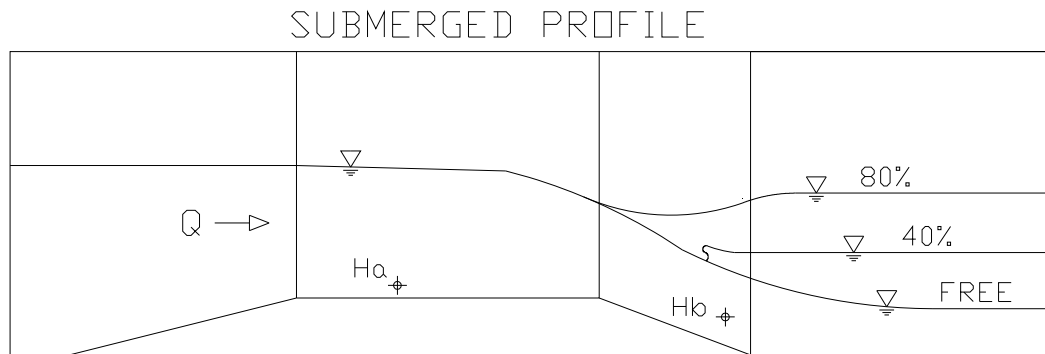


Figure 1. Range of submerged conditions.

free-flow to submerged flow occurs. This can be attributed to the instability of the flow at critical depth, and how the structure behaves hydraulically. Submergence is measured as a ratio of the downstream head,  $H_b$ , to the upstream head,  $H_a$ , and is usually expressed as a percentage (Skogerboe et al. 1967).

## EXPERIMENTAL PROCEDURE

At the Utah Water Research Laboratory in Logan, Utah a 6-in. (15.2 cm) Montana flume was constructed by the original Parshall design specifications (Parshall 1936), but without a diverging section. The constructed Montana flume had a 45-degree entrance wingwalls connecting to the converging section and a 90-degree exit wingwalls downstream of the throat, as was commonly noted during the State of Utah field exercises. A 4:1 horizontal to vertical ramp extended 18 in. (45.7 cm) upstream of the flume. The Montana flume was secured inside a 27 ft (8.13 m) long channel, 37 in. (94 cm) wide, and 24 in. (61 cm) deep. The upstream toe of the ramp was placed 10.5 ft (3.2 m) from the source of flow. A hinge was placed 11.75 ft (3.58 m) downstream of the

flume ramp to increase the submergence (Figure 4). The converging section of the Montana flume was set 4.5 in. (11.4 cm) above the floor of the channel. The level flume was verified by surveying equipment to be within 1/32 in. (0.8 mm) as specified in the Water Measurement Manual (USBR 2001). Water was supplied from a steel pipe by either a 12-in. (30.5 cm) or a 4-in. (10.2 cm) pipeline, depending on the desired flow rate. The 12-in. (30.5 cm) pipeline contained an 8.00 in. (20.3 cm) orifice plate and was calibrated within  $\pm 0.5\%$  accuracy with a weigh tank before testing began. The 4-in. (10.2 cm) pipeline contained a 3.0 in. (7.6 cm) orifice plate that was also calibrated within  $\pm 0.5\%$  accuracy using a weigh tank. Flows were calculated based on the standard orifice equations and a measured pressure differential across the plate.

Six different head measurement devices were installed. One stilling well was placed at the  $H_a$  and  $H_b$  locations on each side of the flume (Figure 3). The port to each stilling well was 5/16 in. (.079 cm) diameter, and was perpendicular to the vertical surface. Plastic tubing, 1/4 in. (0.64 cm) diameter, connected each port to a cylindrical stilling well which was 3/4 in. (3.18 cm) diameter. A ruler with tick marks every 0.1 in. (0.25 cm) was attached to each stilling well using the flumes converging section as an elevation datum. Head measurements on the stilling wells could be measured within  $\pm 0.02$  in. Additional similar rulers were installed as staff gauges to directly measure the water surface elevations at  $H_a$ , and  $H_b$ . The range of flow design for a 6-in. Parshall flume is from 0.05 cfs (0.0014 m<sup>3</sup>/s) to 3.9 cfs (0.110 m<sup>3</sup>/s). Due to physical vertical constraints of the channel where tests were performed, only flow rates up to 3.0 cfs (0.085 m<sup>3</sup>/s) could be measured. Twelve different flow rates were tested during the exercise from 0.25 cfs (0.0071 m<sup>3</sup>/s) to 3.0 cfs (0.085 m<sup>3</sup>/s) increasing by 0.25cfs (0.0071

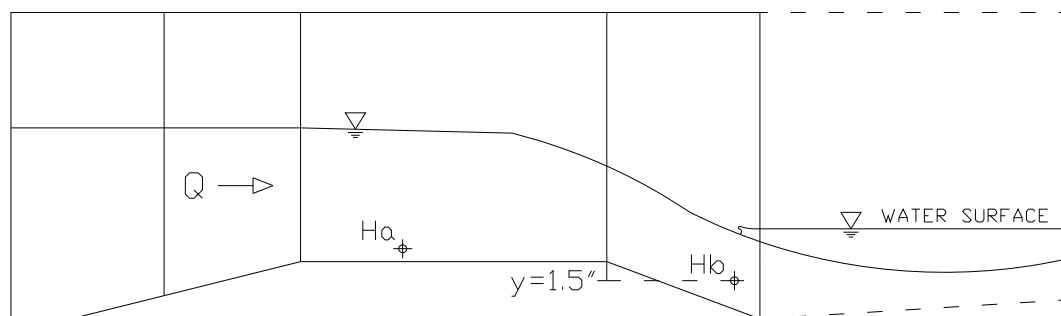


Figure 2. Montana flume side view. Dashed lines represent a Parshall flume.

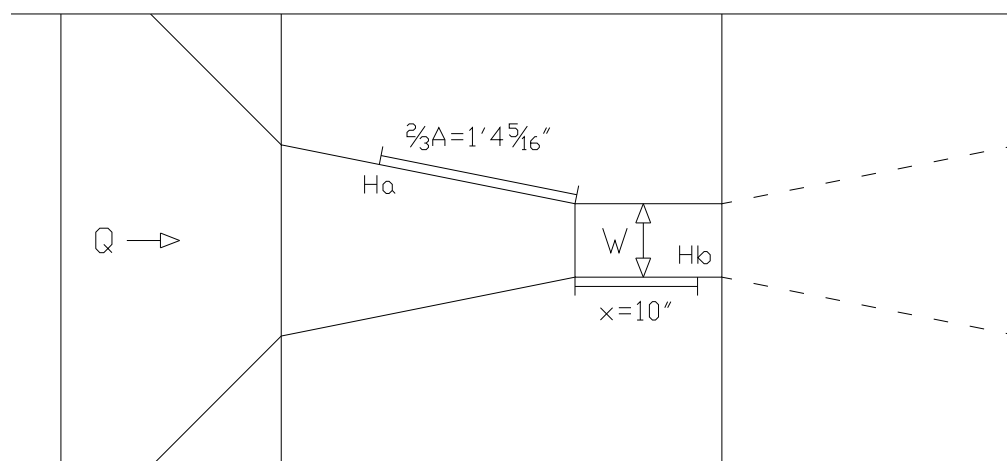


Figure 3. Montana flume plan view. Dashed lines represent a Parshall flume.

$\text{m}^3/\text{s}$ ) for each test. Flow rates from 1.25 cfs ( $0.035 \text{ m}^3/\text{s}$ ) to 3.0 cfs ( $0.085 \text{ m}^3/\text{s}$ ) were supplied from the 12-in. (30.5 cm) pipeline and all flows less than 1.25 cfs ( $0.035 \text{ m}^3/\text{s}$ ) were supplied from the 4-in. (10.2 cm) pipeline. For each flow rate, the upstream head ( $H_a$ ) and downstream head ( $H_b$ ) measurements were collected for a wide range of submergence ( $H_b/H_a * 100$ ) values. If at any time the flow rate changed during testing by more than  $\pm 0.01$  cfs, the flow rate was adjusted back to within that range. Data were

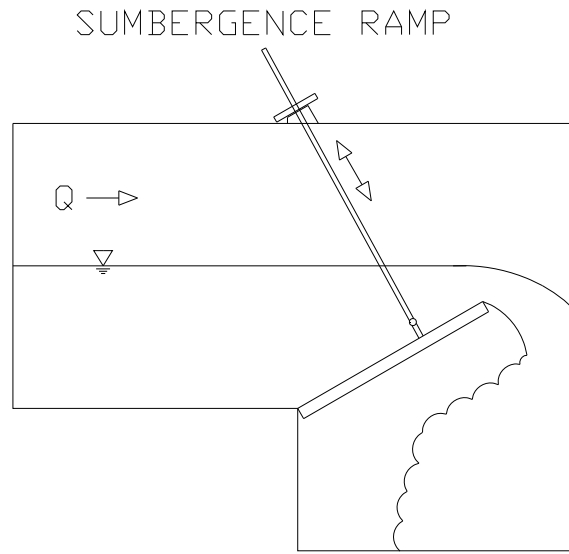


Figure 4. Downstream Ramp to increase submergence.

collected for submergence up to 90%, except for the 3.0 cfs (0.085 m<sup>3</sup>/s) condition at which the channel overtopped. In order to increase the tailwater depth, a ramp at the downstream end of the channel was raised. This was accomplished by raising the thread attached partway up the ramp, as illustrated in Figure 4. Each steady flow rate and tailwater setting was allowed to stabilize for four minutes before readings were taken, even though the head measurement usually stabilized within two minutes.

## RESULTS AND ANALYSIS

*Standard Parshall Rating Table.* Testing revealed that correction factors were necessary in order for the measured test data to correctly estimate the flow through a submerged Montana flume. Standard Parshall equations are customarily used to determine free-flow through a Montana flume as shown in Equation 1.

$$Q = ah_a^b \quad (1)$$

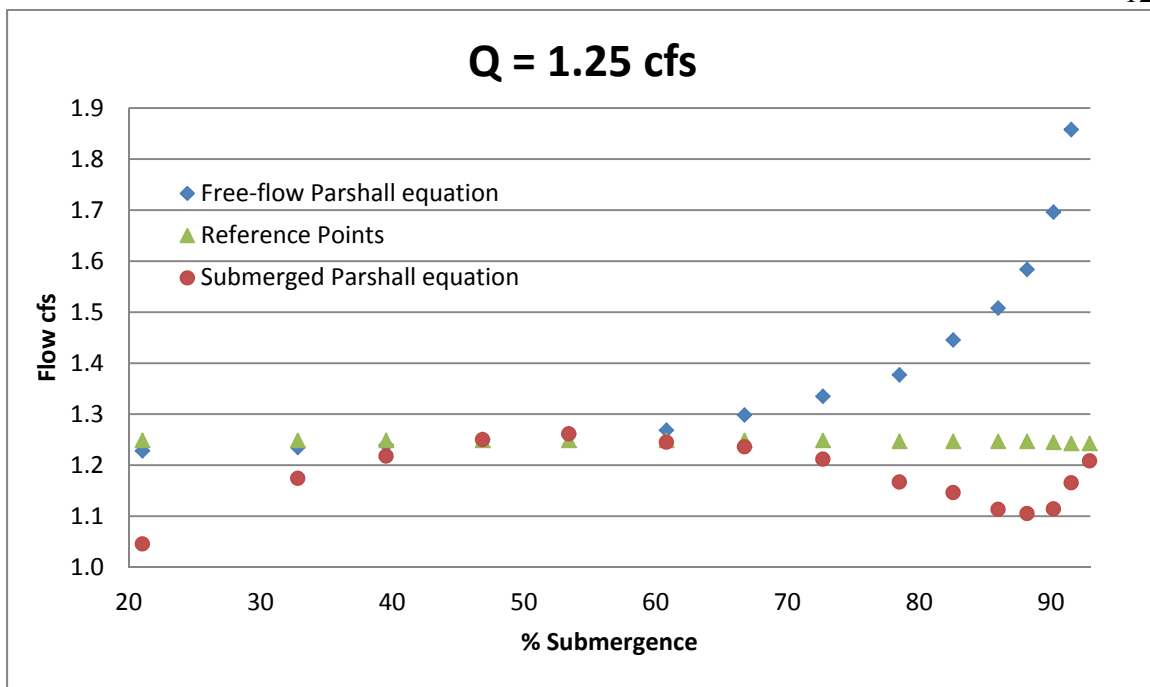


Figure 5. Standard Parshall equations applied to laboratory data.

In a 6-in. flume,  $Q$  is the free-flow rate in cfs;  $a$  is the constant 2.06; and  $b$  is the exponent 1.58. When Equation 1 is applied to a Montana flume, inaccuracies are as high as 48% when submergence reaches 90%. Figure 5 shows the true flow through the flume as calibrated by the actual laboratory flow rate as well as the standard equation applied to the data. These inaccuracies were also noticed by Parshall (1936) during his original testing, and modifications were made to the standard rating table for submergence.

*Parshall Submergence Correction.* In order to correct for inaccuracies due to submergence, Parshall (1936) developed a correction equation when the downstream conditions began to affect the upstream head. When a Parshall flume is operating above 55% submergence, the correction equation is as follows:

$$Q_s = \frac{C_1 * (H_a - H_b)^{n_1}}{[-(\log \frac{H_b}{H_a} + C_2)]^{n_2}} \quad (2)$$

For Equation (2) in a 6-in. (15.2 cm) flume, the constants  $C_1$  and  $C_2$  are 1.66 and .0044, respectively,  $n_1$  and  $n_2$  are 1.58 and 1.080, respectively.  $H_a$  and  $H_b$  are the upstream and downstream head measurements, as previously discussed. When equation 2 is applied to the data collected in this study, the result deviated by as much as 19%. This is shown in Figure 5 as the difference between  $Q_s$  correction and the reference laboratory flow rate. This indicates that a standard Parshall submerged correction cannot accurately be applied to a Montana flume. Due to the diverging geometry, the flow through a Parshall flume will push the hydraulic jump further away from the downstream stilling well  $H_b$ . In a Montana flume, the hydraulic jump is closer to where critical depth occurs in the throat. This causes transitional submergence to be less, as well as increasing the water depth in the downstream stilling well.

*Transition Submergence.* The point when downstream conditions begin to affect the upstream head readings is considered transitional submergence (Skogerboe et al. 1967). For a 6-in. (15.2 cm) Parshall flume, transitional submergence is supposedly reached when  $H_b/H_a * 100$  is greater than 55%. The calculated transitional submergence for the 6-in. (15.2 cm) Montana flume tested in the laboratory is shown in Table 2. The exact values of transitional submergence are difficult to predict and the values in Table 2 are calculations of when the trendline for the free flow Parshall equation separates from the reference flow rate. The average value across all flow ranges is 51% submergence, with some submergence values as low as 42%. This suggests that a Montana flume has a lower transitional submergence value than a Parshall flume. A general trend on all flow

Table 2. Transition submergence for laboratory data

Transition Submergence	
Flow Rate	St
0.25	48
0.51	57
0.76	57
1.00	56
1.25	42
1.51	43
1.75	43
2.00	46
2.25	45
2.49	45
2.75	45
3.00	47
Average	50.6

rates was noted around the transition submergence point. The  $H_b$  ports would oscillate within  $\pm 0.4$  in. alternating sides of the flume. In reading the staff gauge at  $H_b$ , conditions were also unsteady as the flow would surge forward and backward in a cyclic manner (see Appendix A). This unsteady condition near transition submergence was also noted by Skogerboe et al. (1967). The hydraulic jump started to enter the throat near 60% submergence, which is a much lower submergence than when the jump enters the throat on a Parshall flume.

*Testing Summary.* The data given in Figure 6 and 7 was obtained during the laboratory testing. Each flow rate was measured using a calibrated orifice plate in the supply pipeline. Typically, near 50% submergence, the upstream head measurement increased. The flow rates shown are those calculated by Equation 1, based strictly on

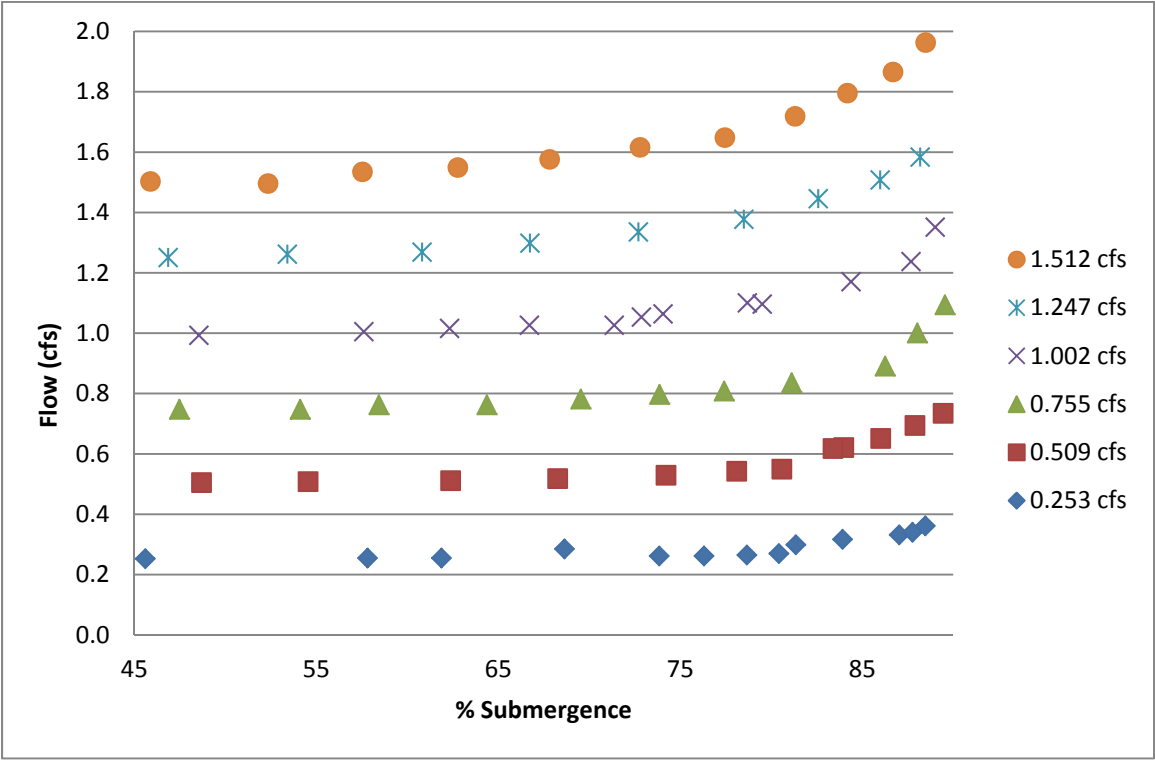


Figure 6. High flow rates for 6-in. (15.2 cm) Montana flume.

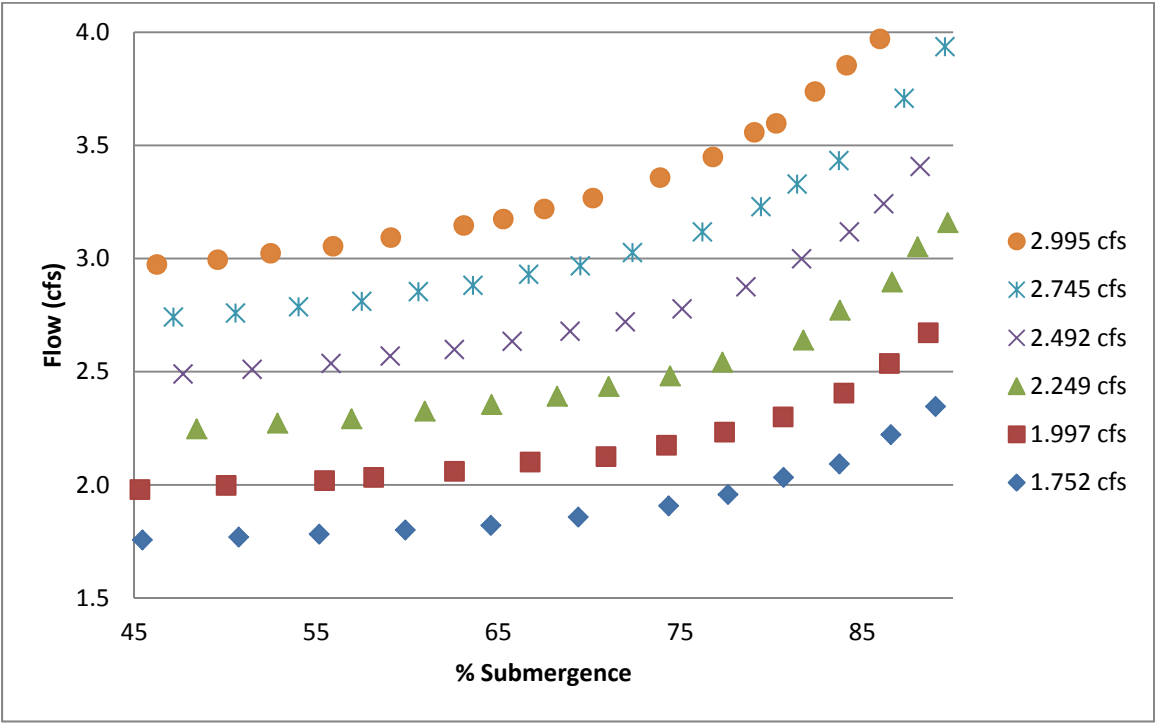


Figure 7. Low flow rates for 6-in. (15.2 cm) Montana flume.



upstream head measurements. Similar curves have been noted for cutthroat flumes under similar submergence conditions (Torres and Merkle 2008).

*Flow Correction.* Adjustments to flow rate can be easily made if the upstream and downstream head measurements are recorded and applied. One approach is to use the standard Parshall equation (Equation 1) to determine the uncorrected flow rate, and the submergence factor ( $H_b/H_a \times 100$ ). This point can be plotted on Figure 6 or 7 and follow the lines parallel to the data points provided to find the adjusted flow rate as demonstrated later in the application section. A second method to determine the true flow rate is to look up the submergence value and interpolate the flow to find a multiplication correction factor,  $\alpha$ , from values given in Table 3. This is also demonstrated in more detail in the application section.

*General Observations.* As seen by Wright and Taheri (1990) when a 1-ft (30.5 cm) Parshall flume was tested under submergence, low discharges had more uncertainty. Wright noticed some discharges to be as far off as 25% from the true value. The smaller flows were more difficult to measure because very small deviations in upstream head could result in large changes in flow calculations. Another difficulty was the transition submergence zone as seen by Skogerboe et al. (1967). Flows in this region are unsteady, and the stilling well readings could oscillate by as much as  $\pm 0.3$  in. (0.76 cm). When this occurred, a general swirling effect in the downstream basin took place. The right and left downstream staff gauges would be offset from each other. When submergence reached close to 60% for lower flows (less than 1.25 cfs), two different flow regimes were noticed. A steady state would be temporarily established, and then the tailwater would wash out and change the downstream head readings. This would occur every six to ten

seconds, shifting between the two states. The two separate readings would occur at one flow rate, with the same downstream submergence ramp height. Appendix A contains photos of this surging condition between the two states.

As the submergence increased, so did the upstream water depth. Due to the increase in water, the flow rate would decrease slightly. The valve was opened by a small degree to maintain a constant flow for all the tests at a specified flow rate. The range of flow never deviated more than 0.05 cfs ( $.001 \text{ m}^3/\text{s}$ ) for any given flow rate.

As anticipated by Heiner (2009), a maximum surface wave of  $\pm 0.6$  in. (1.52 cm) occurred near the upstream 45-degree wingwall as flow entered the flume. Velocities were minimal and the streamlines recovered to their original free surface elevation before the upstream stilling well port or staff gauge. The upstream staff gauge was within  $\pm 0.05$  in. (0.13 cm) of the stilling wells, and the right and left stilling wells were always equal. The downstream staff gauge was nearly never the same reading as the stilling well. Initially, the staff gauge reading was higher than the stilling well, but as submergence increased the stilling well reading was larger. Conditions at the downstream stilling well were unsteady, and regular hydrostatic pressure did not apply. This condition is a large contributing factor to the difference noted in stilling well and staff gauge readings.

The calibration factor for a Montana flume under free-flow conditions slightly under-predicted the flow rate as compared to a Parshall flume. This has been noted by other authors (Abt et al. 1992), but a Parshall flume is rated to be accurate within 3-5%. The under-predictions in flow were all less than 2.3% which is still within an acceptable range.

## APPLICATION

Adjustment factors for submergence were developed but are only applicable when submergence is above the transition submergence found in Table 2. A simple method to determine the correct flow rate for a 6-in. (15.2 cm) submerged Montana flume can be accomplished graphically. The free-flow equation (Equation 1) is first used to find the uncorrected flow rate. The submergence can also be calculated by dividing the downstream head ( $H_b$ ) by the upstream head ( $H_a$ ) and multiplying by 100. Figures 6 and 7 can be used to trace these two values to an intersecting point. An arc can then be drawn that follows parallel between the upper and lower flows. When the Y-axis of the graph is interested, the flow rate can be read.

As an example of correcting the flow rate graphically, Figure 8 is used with  $H_a$  and  $H_b$  as 1.15 ft (35.1 cm) and 0.86 ft (26.2 cm), respectively. Using Equation 1, the flow is calculated as 2.57 cfs (0.073 m<sup>3</sup>/s). The submergence is calculated by dividing  $H_b$  by  $H_a$  and multiplying by 100, giving a value of 75%. By finding where these two values intersect on the graph of flow rates (Figure 6 and 7), and following the curves, an adjusted flow rate is obtained. Using this method a value of approximately 2.31 cfs (0.065 m<sup>3</sup>/s) is obtained as the corrected flow rate.

A second approach is possible through interpolating correction factors. Third order polynomials were used to approximate flows from 0.25 to 3.00 cfs (0.007-0.085 m<sup>3</sup>/s) and had an  $R^2$  value greater than 0.96. Table 3 can be used to interpolate between flows by using the given submergence value. The polynomial approximations are only valid for submergence from 45 to 90%. Due to physical limitations of the channel where tests were performed, values for 3.00 cfs (0.085 m<sup>3</sup>/s) could only be obtain for up to 87%

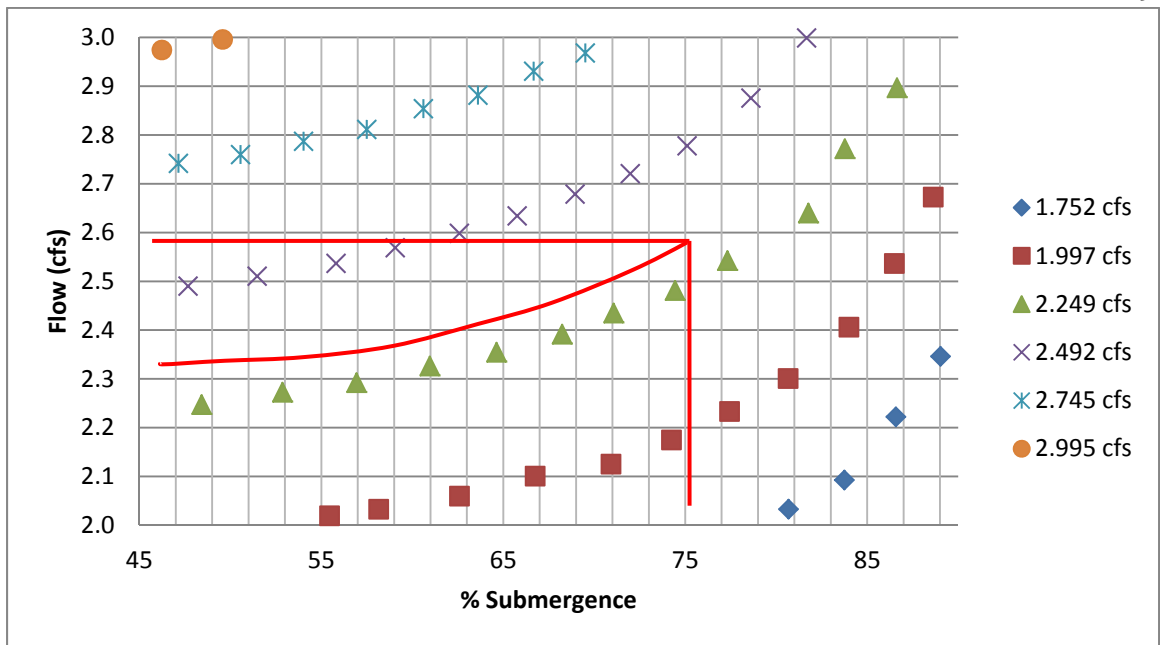


Figure 8. Graphical correction for laboratory data.

Table 3. Correction factors based on laboratory data

Flow rate cfs	0.25	0.51	0.76	1.00	1.25	1.51	1.75	2.00	2.25	2.49	2.75	3.00
Submergence												
45	1.002	1.012	1.011	1.014	0.991	0.998	0.992	1.003	1.000	0.999	1.000	1.005
48	1.000	1.010	1.009	1.011	0.985	0.997	0.984	0.993	0.991	0.989	0.991	0.998
51	0.998	1.007	1.007	1.007	0.983	0.996	0.980	0.987	0.984	0.982	0.985	0.991
54	0.996	1.004	1.004	1.002	0.982	0.995	0.978	0.983	0.980	0.978	0.980	0.984
57	0.993	1.000	1.000	0.997	0.982	0.994	0.977	0.981	0.977	0.974	0.975	0.977
60	0.991	0.996	0.995	0.992	0.982	0.991	0.975	0.978	0.973	0.970	0.969	0.969
63	0.987	0.990	0.990	0.986	0.980	0.985	0.972	0.974	0.967	0.964	0.961	0.958
66	0.983	0.984	0.984	0.980	0.974	0.977	0.966	0.967	0.958	0.955	0.950	0.944
69	0.979	0.977	0.978	0.973	0.965	0.965	0.955	0.956	0.946	0.941	0.935	0.926
72	0.973	0.970	0.970	0.962	0.952	0.948	0.939	0.940	0.928	0.923	0.915	0.905
75	0.966	0.960	0.962	0.949	0.932	0.927	0.918	0.918	0.905	0.899	0.890	0.880
78	0.941	0.937	0.950	0.933	0.907	0.902	0.891	0.890	0.877	0.869	0.860	0.851
81	0.888	0.888	0.910	0.896	0.876	0.872	0.858	0.856	0.843	0.834	0.825	0.818
84	0.811	0.826	0.851	0.842	0.839	0.839	0.820	0.816	0.804	0.793	0.786	0.782
87	0.744	0.754	0.776	0.777	0.798	0.802	0.777	0.772	0.761	0.749	0.743	0.743
90	0.697	0.677	0.692	0.705	0.753	0.762	0.731	0.725	0.715	0.703	0.699	0.703

submerged. Flow rates are obtained using Equation 1 and are then multiplied by the correction factor,  $\alpha$ , in the table. If the same values of  $H_a$  and  $H_b$  are taken as 1.15 and 0.85 as in the graphical approach, the uncorrected flow rate would be 2.57 cfs (0.073 m<sup>3</sup>/s) with a submergence of 75%. By linear interpolation the correction coefficient,  $\alpha$ , is 0.896. The corrected flow rate is obtained by multiplying the flow rate by the correction factor, providing a result of 2.30 cfs (0.065 m<sup>3</sup>/s). The graphical and interpolation methods yield similar results.

## CONCLUSIONS

The results from this research demonstrate that the Parshall flume rating table may be used for free-flow Montana flumes. The Parshall rating table used for submergence corrections, however, cannot be used if the 3-5% accuracy indicated by Parshall (1936) is to be achieved. Transition submergence is also less for a Montana flume (51%) than a Parshall flume (55%). This means that the downstream depth does not need to be as high in order to affect the upstream head measurements. Correction coefficients and methods of correcting flow are provided for a 6-in. Montana flume with 45-degree entrance wing walls and 90-degree exit wing walls. A graphical and an interpolation method are demonstrated which yield similar results. The correction factors presented herein are only valid for a smooth, level flume with a submergence of 45-90%.

## CHAPTER III

USING *FLOW 3D*<sup>TM</sup> TO CORRECT FLOW RATES FOR A SUBMERGED  
MONTANA FLUME<sup>2</sup>**ABSTRACT**

A numerical model was created of a 6-in. Montana flume to replicate the measurement structure created to collect laboratory data. Wing walls of 45-degrees were developed upstream as well as a 4:1 horizontal to vertical ramp. Perpendicular wingwalls were placed on the downstream section of the throat. Steps are outlined to create a working model in *Flow 3D*<sup>TM</sup> by using a nested meshing system. Initial water surface elevations were also included to maximize simulation efficiency. Upstream and downstream head measurements were measured for a variety of flow rates and submerged conditions by means of stilling wells. Symmetry was applied when possible to reduce the computational demand. The standard Parshall rating curve may be used for free-flowing Montana flumes. Errors up to 48% were calculated when the standard Parshall rating curve was applied to the submerged data. Adjustment factors for submerged Parshall flumes cannot be applied to Montana flumes where deviations were as high as 18% from the actual flow rate. Steps are outlined to create a working model in *Flow 3D*<sup>TM</sup>. Correction factors for a 6-in. Montana flume are provided graphically as well as in a tabular format. 91% of the data collected from the numerical model deviated from the laboratory data by  $\pm 4.0\%$ .

---

<sup>2</sup> Coauthored by Ryan Willeitner and Steven L. Barfuss, P.E.

## INTRODUCTION

Physical models are one method to test submergence in an open-channel measurement device; however, they can be tedious to design, require large spaces, and are time consuming to build. Models can also be very expensive and stabilization time can be very long. Davis and Deutsch (1980) developed a three-dimensional finite-difference program to numerically predict flows through a 6-in. (15.2 cm) Parshall flume. The testing was initially begun so predictions could be made for alterations in channel slope, upstream velocity profile distortions, and flume geometry. One of the largest differences between the numerical model and the experiment was the lack of viscosity in the numerical method. A substantial drawback to the study was “the availability of sufficient computer resources.” Thirty years later, computer resources are much more plentiful. *Flow 3D*<sup>TM</sup> version 9.4 is a Computational Fluid Dynamics (CFD) software that allows the user to simulate models with computing power that leads to quick, highly accurate results.

During field testing for the state of Utah, it took an average of three hours to validate one particular flow rate. By using a CFD program, the dimensions of a measurement device could be taken, and an entire free-flow rating table could be developed in the same time it would take the user to verify one point. Constant canal cross sections could also be calibrated quickly without ever having to change the flow rate.

## EXPERIMENTAL PROCEDURE

There were eight steps necessary to produce the information presented in this paper. The several versions of *Flow 3D*<sup>TM</sup> have unique options, and the steps used are for version 9.4 although other versions may be similar. These steps apply to a 6-in. Montana flume whereas other sizes or shapes of flumes may need additional considerations.

Step 1 Model: A properly scaled model needs to be constructed which can be accomplished in *Flow 3D*<sup>TM</sup>, however, the interface is less user friendly and more cumbersome than a software package such as *AutoCad*<sup>TM</sup>. If creating the model in a program other than *Flow 3D*<sup>TM</sup>, the shape can be exported as an STL file to be properly imported into *Flow 3D*<sup>TM</sup>. When exported from a drafting program, the model was scaled to feet measurements for simplicity and ease of conversions. The 6-in. (15.2 cm) Montana flume was designed according to the dimensions developed by Parshall (1936) for a 6-in. (15.2 cm) flume without a diverging section. The upstream wingwalls were at 45 degrees and a 4:1 horizontal to vertical ramp extended vertically 4.5 in. (11.4 cm) to meet the converging section of the flume. The wing walls were limited to three feet wide and the entire flume was extended 3 feet vertical of the flumes converging section. The downstream wingwalls were created at 90-degrees to the channel walls. No walls on the channel need be created in the model because those surfaces will be simulated with boundary conditions. However, extensions should be made some distance upstream and downstream. The author chose to use half a foot of channel upstream of the wing walls and three feet of downstream of the throat to properly simulate laboratory conditions. Hirt and Williams (1994) used 0.75 feet (22.9 cm) of channel upstream and downstream of a Parshall flume to test for submergence, but this was inadequate distance for a



Montana flume under submergence. Stilling well ports of 5/16 in. (0.79 cm) diameter were placed at the proper upstream and downstream head locations. Sufficient numerical nested meshing must be able to fit inside the stilling well ports to properly calculate flow (see Step 5 Meshing and Geometry Tab).

Step 2 General Tab: Each run was set to compute for 25 seconds. This allowed the system to stabilize and also remain stable for some time. Most stabilization occurred within 10-15 seconds because of optimization techniques described in the Boundaries and Initial Tabs. Initially simulations were performed at single precision for higher accuracy, but this was unnecessary due to the size and method of meshing. Using four quad core processors (16 total), runs at single precision would take approximately 5 hours and 20 minutes. When double precision was selected, the same accuracy was obtained, but simulations processed in less than 2 hours. Head measurements for the standard Parshall rating equations (Equation 1) are based on feet, therefore the units were changed to Engineering Units (feet, slugs, seconds). The system is constantly exposed to atmospheric pressure so a single fluid was set to be incompressible.

Step 3 Physics Tab: Only two types of physics were applied to this model setup. Gravity was established as negative 32.2 feet per second squared ( $9.81 \text{ m/s}^2$ ) in the downward coordinate (-z). The fluid in the model was also set as a viscous Newtonian fluid with the renormalized group RNG radio button selected due to high turbulence (*Flow 3D*<sup>TM</sup> User Manual). Wall shear stresses were neglected because of minimal effects they had on the flow rate.

Step 4 Fluids Tab: Water at 20 degrees Celsius was imported from the database, and the units were transferred into Engineering. This gives a kinematic viscosity of the

water of 2.0886 E-5 pound second per foot squared. Several different sections of fluid were used (see Initial Tab), but all of them were based off these same fluid properties. All other options were kept to their default settings.

Step 5 Meshing and Geometry Tab: The most difficult part of the model was creating an appropriate mesh. If the mesh was too small, the calculations would take a very long time. On the other hand, a large mesh would not give the accuracy needed to perform a detailed analysis. Many levels of access are available with *Flow 3D*<sup>TM</sup>. Originally this project was started with the education version which only allotted 200,000 total mesh cells. This was insufficient to properly simulate a large section of channel as well as a very small diameter stilling well port. For an accurate calculation to take place, at least six full mesh cells need to be calculated for any point in the flow (*Flow 3D*<sup>TM</sup> User Manual). To replicate the laboratory data, the stilling well ports needed to be 5/16 in. (0.79 cm) diameter, which is a very fine mesh. A series of nested meshes were developed to allow for minimal total cells, as well as high precision where needed. The largest mesh was half the width (assuming symmetry) and the full height of the channel extending from the upstream ramp to two feet downstream of the throat. The length of each side in the cubic cell was set to 0.10 feet (3.05 cm). A second nested mesh was placed inside the first extending the full height of the flume, but only the width of the actual flume. The wing walls are not considered part of the flume. The second mesh extended downstream of the throat for 0.75 feet (22.9 cm) to properly simulate the tailwater reentering the throat with cubic cell lengths of 0.05 feet (1.52 cm). Two small meshes were developed at each stilling well port extending 0.2 feet (6.10 cm) from the vertical face towards the inside of the flume, and 0.1 feet (3.05 cm) into the stilling well.

These small meshes were set to a cubic cell size of 0.01 feet (0.305 cm) so the cross section of the ports had eight full cells to properly calculate flow. Fixed points were inserted in each mesh along the length of the flume whenever one mesh intersected another. The fixed points helped to optimize continuity between meshes and provide more accurate calculations. See Appendix B for images of meshing and geometry.

Step 6 Boundaries Tab: A great advantage of a Montana flume is the symmetry that can be applied along the length. Symmetry was also applied between meshes as well as for walls of the channel. A symmetrical boundary condition acts like a mirror and reflects the flow similar to a wall. The only locations where symmetry did not apply were the entrance, and exit of the largest mesh. A volumetric flow rate was set at the entrance as well as an anticipated height of flow. A system of equations was established to convert the laboratory data from chapter II to estimated upstream and downstream depths. The F Fraction is a variable to determine the ability of a liquid to pass through a boundary and was set to one enabling the upstream and downstream flow to pass through freely. The downstream boundary was established as a specified pressure height which maintained a constant water depth. Laboratory data is not essential because submergences resulted in different values. The only advantage to using the laboratory data was to quickly establish a consistent increase in submergence without having to view results of previous tests.

Step 7 Initial Tab: To maximize efficiency and decrease run time, two separate water surfaces were initially set in the flume (Hirt and Williams 1994). It took a longer time for the stilling wells to stabilize than the rest of the flume, so the stilling well depths were anticipated and set to near stabilized conditions from the start. Without this water

surface in place, many of the simulations were aborted early due to large deviations between cells at these higher flow rates. See Appendix B for initial water surface profiles.

Step 8 Output and Numerics Tabs: Not all data was needed, so only hydraulic data, and particle information for two- and three-dimensional plots were selected. To better estimate stabilized conditions, data was recorded at 0.75-second increments. A first order momentum advection was used for calculations. The fluid flow solver was set to compute based on momentum and continuity equations. The pressure solver options were also set to implicit as recommended by the *Flow 3D*<sup>TM</sup> User Manual.

## **RESULTS AND ANALYSIS**

*Obtaining Results.* The Analyze tab in *Flow 3D*<sup>TM</sup> is the location to gather testing information. When selecting Hydraulic data in Step 8 of the setup, the fluid depth, and free surface elevation options were made available. For this project, the free surface fluid elevation was read from the stilling wells, and the height of the converging section was subtracted. This method was used because the Hb stilling well port is below the converging section height. If fluid depth was measured, it would be a value greater than what was modeled in the laboratory. A probe at the center of each stilling well was used to collect data. Data points were created every 0.75 seconds for a total of 25 seconds. 90% of all the flows would stabilize from 6 to 16 seconds. The last 5 seconds of the 25-second run were averaged to obtain upstream and downstream stilling well fluid depths. If the flows deviated more than 0.01 feet (0.305 cm) in the last five seconds, the simulation was continued for an additional 5 seconds. All tests had stabilized within 0.01

feet (0.305 cm) in 30 seconds, and an average was taken from 25 to 30 seconds as the stilling well depth. Three-dimensional flow simulations could also be viewed in the Display tab, but these proved unhelpful to retrieve accurate consistent data.

*Testing Summary.* The data collected in Figures 9 and 10 is a summary of the information collected during testing. Only submergence from 45-90% is posted because those are the values where submergence had an effect on the flow rates tested during this study. On average, 10 tests were recorded at each flow rate. All flow rates are designated in the legend and are in units of cfs. The flow rates indicated are based on the standard Parshall equation (Equation 1) for a 6-in. (15.2 cm) Parshall flume, and are based solely on the upstream head. The percent submergence is a ratio of downstream head to upstream head given as a percentage. Calculated flow rates deviate from the actual flow rates as much as 48%. When the submerged Parshall adjustment factors

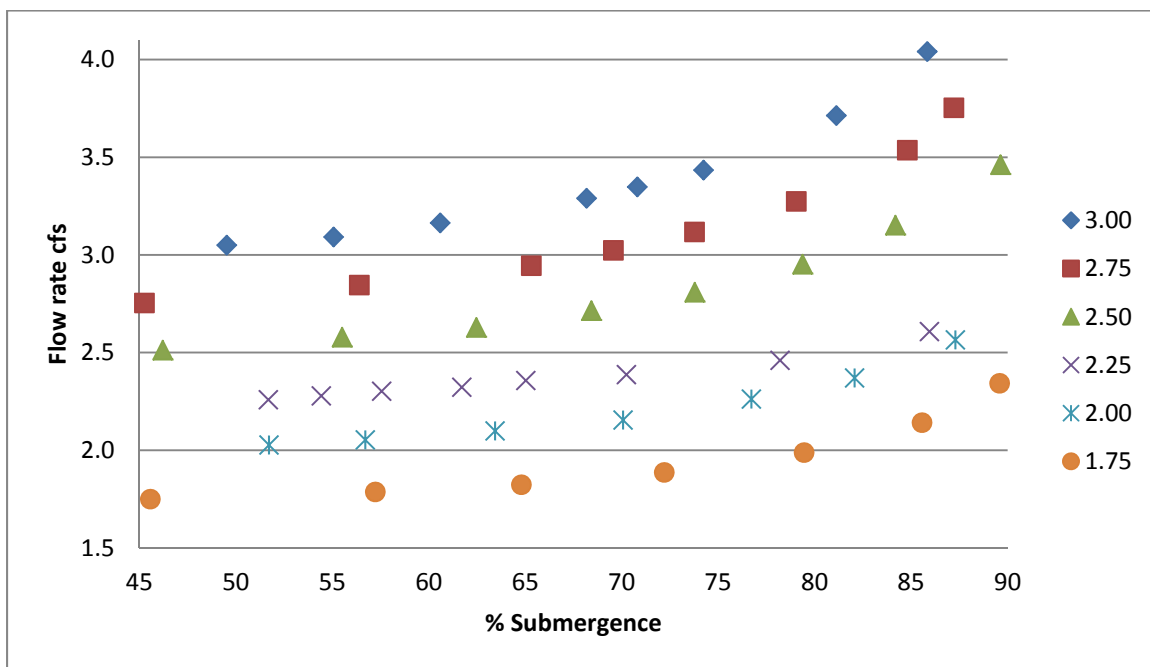


Figure 9. High flow rates using *Flow 3D*<sup>TM</sup>.

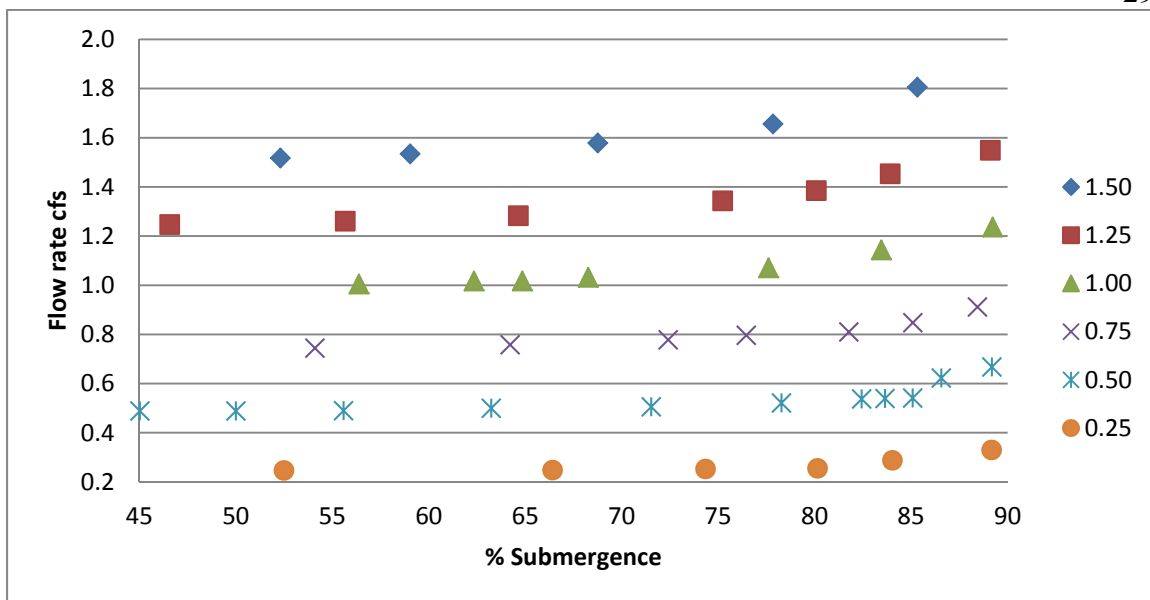


Figure 10. Low flow rates using *Flow 3D*<sup>TM</sup>.

(Equation 2) were applied to the data, deviations up to 18% were calculated.

*Laboratory Data Compared to Numerical Data.* Third order polynomial trendline equations were developed to approximate the data collected with  $R^2$  values above 0.99. This data is limited to 45-90% submergence because of instabilities in the equations at percentages above 90. Laboratory data was adjusted to compensate for minor deviations between the target flow and actual flow and then compared to the numerical data. The target flow for the numerical data is also the actual flow. Numerical data deviations from the laboratory data are summarized in Table 4. 91% of all data points collected numerically were within  $\pm 4.0\%$  of the laboratory data results. It is noted that the highest deviations are with low flows and high submergence as anticipated in literature. Wright and Taheri (1990) noted that low flow rates had high deviations when submergence levels were large. Very small changes in head result in large flow differences. It is noted

Table 4. Percent deviation from laboratory data to numerical data

Flow cfs	0.25	0.50	0.75	1.00	1.25	1.50	1.75	2.00	2.25	2.50	2.75	3.00
Submergence												
45	-1.08	-1.78	-0.42	2.47	0.71	0.48	0.65	1.98	2.19	2.23	1.72	2.03
48	-1.28	-2.21	-0.32	2.67	0.54	0.94	0.80	1.48	2.12	1.99	1.44	2.69
51	-1.51	-2.35	-0.18	2.57	0.51	1.29	0.98	1.40	2.10	1.98	1.52	3.10
54	-1.75	-2.28	-0.03	2.27	0.58	1.52	1.16	1.64	2.10	2.14	1.85	3.30
57	-1.98	-2.10	0.11	1.85	0.72	1.66	1.33	2.09	2.15	2.42	2.34	3.34
60	-2.18	-1.89	0.22	1.41	0.89	1.70	1.47	2.66	2.22	2.76	2.87	3.27
63	-2.34	-1.74	0.41	1.13	1.05	1.66	1.58	3.24	2.32	3.10	3.35	3.13
66	-2.43	-1.74	0.72	1.04	1.17	1.54	1.62	3.74	2.45	3.40	3.68	2.98
69	-2.43	-1.97	1.02	1.07	1.21	1.36	1.60	4.05	2.60	3.59	3.75	2.85
72	-2.32	-1.92	1.29	1.10	1.14	1.13	1.49	4.07	2.76	3.62	3.01	2.79
75	-3.31	-1.85	1.55	1.42	0.93	0.86	1.29	3.73	2.93	3.46	2.08	2.83
78	-3.53	-3.25	1.57	1.91	0.55	0.56	0.99	2.97	3.11	3.07	1.43	3.01
81	-5.04	-5.85	-1.33	0.64	0.00	0.26	0.59	1.75	3.27	2.43	1.27	3.33
84	-7.98	-7.66	-5.97	-2.28	-0.72	-0.04	0.11	1.13	3.43	1.56	1.78	3.83
87	-8.81	-7.82	-9.34	-6.20	-1.60	-0.33	-0.44	1.36	3.57	0.46	3.05	4.49
90	-6.15	-5.90	-11.5	-10.9	-2.63	-0.58	-1.06	2.08	3.69	-0.83	5.12	5.31

that the highest deviations were at low flows and high submergence validating Wrights conclusions.

*General Observations.* Numerical simulations generally followed what was observed during the laboratory testing. Some flow rates however, would be established for a few seconds, then suddenly increase due to a wave propagating into the throat. This was noted for similar flow rates at specific submergence levels in both the laboratory and numerical models. For consistency, the minimum head measurement was recorded for both laboratory and numerical data. These subtle similarities give evidence that the setup conditions were appropriate for the testing performed.

Some warnings and errors were encountered during the testing procedure. When submergence levels rose over 93%, a “persistent f-packing” problem within the

*Flow3D*<sup>TM</sup> software caused the simulation to abort prematurely. Data was only desired up to 90% submergence so these simulations were discarded. At flows below 0.75 cfs (0.021 m<sup>3</sup>/s), an “excessive pressure convergence failure” notice appeared which also resulted in a premature end to the simulation. This was resolved however, by increasing the fine mesh size around the downstream stilling well port.

When a flow rate of 3.00cfs (0.085 m<sup>3</sup>/s) and a submergence of 90% was simulated, the initialized water surface condition converged more than three times faster than un-initialized. The upstream boundary height seemed to have little effect on the results. Small changes in the downstream boundary depth, however, had very large effects on the submergence.

The author spent approximately 150 hours designing, building, installing, and testing the physical model. Approximately 50 hours were spent learning *Flow 3D*<sup>TM</sup>, troubleshooting errors, and retrieving results from simulations. This illustrates how much more efficient in time a numerical model can be in comparison to laboratory data collection. It is anticipated that alternate size Montana flume could be calibrated for submergence by the methods provided within 20 hours by using *Flow 3D*<sup>TM</sup>.

## **APPLICATION**

A simple method for finding the accurate flow rate for a 6-in. (15.2 cm) submerged Montana flume can be accomplished graphically. The free-flow equation (Equation 1) is first used to find the uncorrected flow rate. The submergence also is then found by dividing the downstream head ( $H_b$ ) by the upstream head ( $H_a$ ) and multiplying by 100. Figures 9 and 10 can be used to trace these two values to an intersecting point.



An arc can be drawn parallel between the upper and lower flows provided. The flow rate can be read from the left side of the graph where the arc intersects the Y-axis.

Figure 11 demonstrates how to graphically estimate flow corrections. As an example,  $H_a$  and  $H_b$  are given as 1.15 ft (35.1 cm) and 0.86 ft (26.2 cm), respectively. By using Equation 1 the standard Parshall equation calculates a flow rate of 2.57cfs (0.073 m<sup>3</sup>/s). By dividing  $H_b$  by  $H_a$  and multiplying by 100, a submergence factor of 75% is calculated. By finding where these two values intersect on the graph of flow rates (Figure 9 and 10), and following the curves parallel to the Y-axis, an adjusted flow rate is obtained. This is demonstrated in Figure 11, and a value of approximately 2.28 cfs (0.065 m<sup>3</sup>/s) is obtained. A second approach is by interpolating correction factors. Third order polynomials were used to approximate flow rates. Where  $R^2$  values were below 0.90 two piece-wise third order polynomials were used for approximations, which resulted in  $R^2$

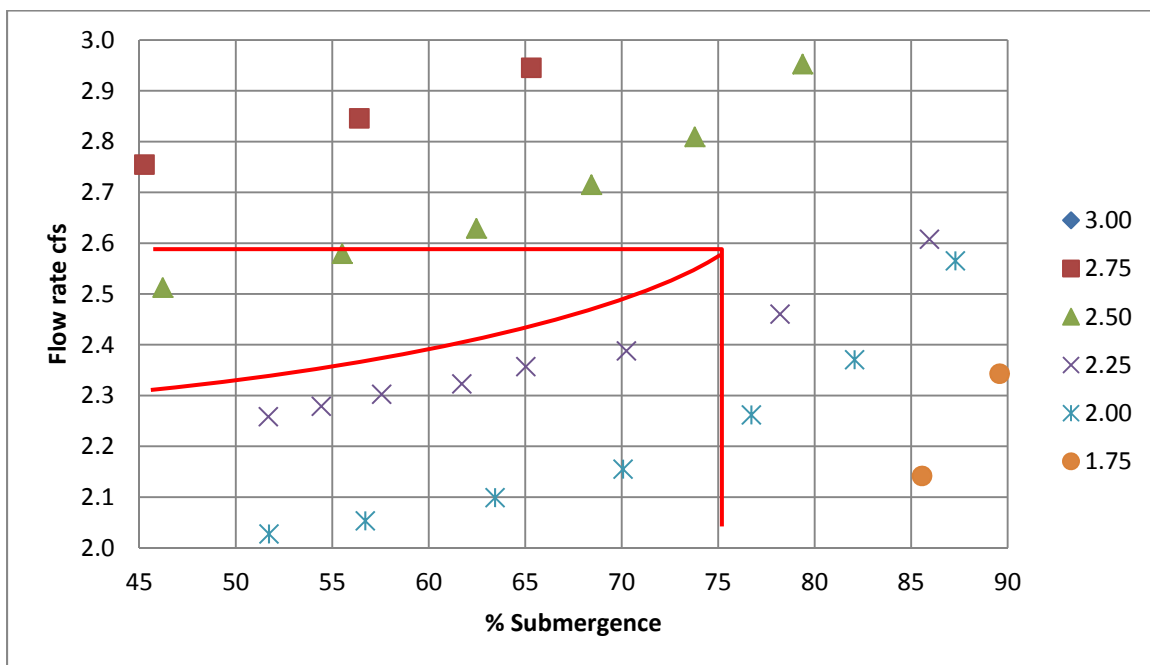


Figure 11. Graphical correction for numerical data.

Table 5. Correction factors for numerical data

Flow cfs	0.25	0.50	0.75	1.00	1.25	1.50	1.75	2.00	2.25	2.50	2.75	3.00
Submergence												
45	1.013	1.024	1.021	0.999	0.998	0.997	0.996	0.997	0.991	0.992	0.997	0.999
48	1.013	1.023	1.018	0.994	0.994	0.991	0.987	0.992	0.982	0.985	0.991	0.985
51	1.013	1.021	1.014	0.991	0.992	0.987	0.981	0.986	0.976	0.978	0.983	0.974
54	1.013	1.018	1.010	0.990	0.991	0.984	0.978	0.980	0.972	0.972	0.975	0.966
57	1.013	1.015	1.004	0.989	0.989	0.982	0.975	0.974	0.968	0.966	0.966	0.959
60	1.013	1.009	0.998	0.988	0.987	0.978	0.972	0.966	0.963	0.959	0.955	0.951
63	1.011	1.002	0.991	0.985	0.983	0.973	0.967	0.956	0.957	0.949	0.943	0.941
66	1.008	0.996	0.982	0.980	0.977	0.966	0.960	0.945	0.947	0.937	0.929	0.929
69	1.004	0.991	0.973	0.972	0.968	0.955	0.950	0.931	0.933	0.923	0.913	0.913
72	0.995	0.983	0.963	0.961	0.954	0.941	0.936	0.915	0.914	0.904	0.900	0.892
75	0.983	0.973	0.952	0.945	0.937	0.923	0.916	0.897	0.890	0.882	0.884	0.867
78	0.962	0.962	0.940	0.925	0.915	0.901	0.892	0.876	0.861	0.856	0.859	0.837
81	0.932	0.938	0.927	0.900	0.888	0.874	0.862	0.852	0.826	0.826	0.826	0.802
84	0.882	0.889	0.910	0.870	0.858	0.843	0.827	0.818	0.787	0.793	0.783	0.763
87	0.816	0.813	0.861	0.836	0.823	0.808	0.789	0.772	0.744	0.757	0.731	0.721
90	0.742	0.715	0.786	0.799	0.785	0.770	0.746	0.720	0.698	0.719	0.674	0.677

values above 0.99. Table 5 can be used to interpolate between flows by using the given submergence value. The polynomial approximations are only valid for submergence from 45 to 90%. Flow rates are obtained using Equation 1 and are then multiplied by the correction factor  $\alpha$  in Table 5. If the same values of  $H_a$  and  $H_b$  are taken as 1.15 and 0.85 as in the graphical approach, the uncorrected flow rate would be 2.57 cfs (0.073 m<sup>3</sup>/s) and submergence of 75%. By linear interpolation we have a correction coefficient  $\alpha$  of 0.882. The corrected flow rate would be obtained by multiplying the flow rate by the correction factor providing a result of 2.27 cfs (0.064 m<sup>3</sup>/s). The graphical and interpolation methods yield similar results. The numerical data and laboratory data also provide solutions within 2% of each other.

## CONCLUSIONS

With ever increasing advancements in technology, and when the application is appropriate, computational fluid dynamic software is able to match physical modeling, and usually requires less time to collect data. As demonstrated herein, accuracies of CFD programs is reliable, even for complicated systems with submerged flow. Device specific calibrations cannot be applied to all other similar devices as in the case of Parshall and Montana flumes. Although geometries are similar and free-flow conditions are the same, these two flumes cannot use the same corrections for submergence.

Numerical testing for the 6-in. (15.2 cm) Montana flume proved to deviate from the laboratory data by  $\pm 4.0\%$  for 91% of all data points collected. This is an acceptable accuracy compared to Parshall's (1936) original 3-5% accuracy. The largest of these deviations were at flows below 1.00 cfs (0.028 m<sup>3</sup>/s) and submergence above 75%. Simple methods of establishing a corrected flow rate have been presented both graphically and by linear interpolation for a 6-in. (15.2 cm) Montana flume.

The numerical method was three times more efficient in time for the user than collecting laboratory data. This time efficiency is a major advantage of numerical modeling. The required time to develop a submerged rating table for another sized Montana flume would be about the same as for a 6-in. (15.2 cm) flume. The numerical method of modeling becomes much more efficient with regard to time than by using physical models.

## CHAPTER IV

## SUMMARY AND CONCLUSIONS

To assist the state in regulating water throughout Utah, a study was conducted on open-channel and closed conduit measuring devices. Geometric problems were found with the measuring devices which include Parshall flumes. Some of the Parshall flumes had no diverging section and are referred to as Montana flumes. Free-flow equations for Parshall flumes can be used with Montana flumes, but submergence corrections do not.

A traditional physical modeling approach was taken to create a new rating table for submerged Montana flumes. A 6-in. (15.2 cm) Montana flume was created to design specifications, and tested under various flows and submerged conditions. Errors up to 16% were calculated when the laboratory data was compared to corrections for a submerged Parshall flume. Correction factors were given for flow rates up to 3.0 cfs (0.085 m<sup>3</sup>/s) in a graphical and tabular format.

The laboratory data was validated through a computational fluid dynamics software program called *Flow 3D*<sup>TM</sup>. When compared to this numerical data, errors up to 18% were calculated compared to flow for a submerged Parshall flume. 98% of all the data points collected in the numeric model were within  $\pm 2.5\%$  of the lab data.

The same numerical method for developing submergence curves could also be applied to other sized Montana flumes. Other open-channel structures can be calibrated by using a computational fluid dynamics software.

## CHAPTER V

## FUTURE RESEARCH

Throughout the state of Utah, many open-channel and closed-conduit measurement devices have been tested and found to be outside of their design accuracy specifications. The information presented in this thesis indicates that modified geometries significantly affect flow measurement accuracies. By maintaining measurement structures, and ensuring proper geometry, accuracies can be within the design specifications.

A computational fluid dynamics software program, such as *Flow 3D*<sup>TM</sup>, can be used to create rating tables for a wide range of measurement structures. By using this kind of software, space and time commitments can be significantly reduced and still provide satisfactory results. Methods of obtaining efficient and accurate submergence data are outlined in Chapter III. This can be applied to the entire size range of Montana flumes which are found in the field. Appropriate meshing will change with the size of each flume demanding a reined meshing system, but other methods should remain the same.

## REFERENCES

- Abt, S.R., Cook, C., Staker, K.J., and Johns, D.D. (1992). "Small Parshall flume rating correction." *J. Hydr. Engrg.*, ASCE, 118(5), 198-803.
- Abt, S.R., Florentin, C.B., Genovez, A., Ruth, B.C. (1995). "Settlement and submergence adjustments for Parshall flume." *J. Irrig. Drain. Engrg.*, ASCE, 121(5), 317-321.
- Abt, S.R., Genovez, A., and Florentin, B. (1994). "Correction for settlement in submerged Parshall flumes." *J. Irrig. Drain. Engrg.*, ASCE, 120(3), 676-682.
- Davis, R.W., and Deutsch, S. (1980). "A numerical-experimental study of Parshall flumes." *J. Hydr. Res.*, 18(2), 135-151.
- Genovez, A., Abt, S., Florentin, B., and Garton, A. (1993). "Correction for settlement in a Parshall flume." *J. Irrig. Drain. Engrg.*, ASCE, 119(6), 1081-1091.
- Heiner, Bryan (2009). "Parshall flume staff gauge location and entrance wingwall discharge calibration corrections." Thesis, Utah State Univ., Logan, Utah.
- Hirt, C.W., and Williams, K.A. (1994). "Flow-3D predictions for free discharge and submerged Parshall flumes." *Flow Science, Inc.* FSI-94-TN40.
- Parshall, R.L. (1936). "The Parshall measuring flume." *Bull. No. 423*, Agric. Experiment Station, Colorado Agric. Coll., Fort Collins, Colo., Mar.
- Robinson, A.R. (1965). "Simplified flow corrections for Parshall flumes under submerged conditions." *Civ Engrg.*, ASCE, 25(9), 75.
- Skogerboe, G.V., Hyatt, M.L., England, J.D., and Johnson, J.L. (1967). "Design and calibration of submerged open channel flow measurement structures. Part 2: Parshall flumes." *Rep. WG31-3*, Utah Water Res. Lab., Utah State Univ., Logan, Utah.
- Torres, A.F., Merkley, G.P. (2008). "Cutthroat Measurement Flume Calibration for Free and submerged Flow Using a Single Equation." *J. Irrig. and Drain. Engrg.* 134(4)
- U. S. Department of the Interior, Bureau of Reclamation (USBR). (2001). *Water measurement manual* 3rd ed., U.S. Government Printing Office, Washington, D.C.
- U. S. Department of the Interior, Bureau of Reclamation (USBR). (2007). *Water operation and maintenance Bull. No. 180*, U.S. Government Printing Office, Washington, D.C.

Wright, S.J., and Taheri, B. (1990). "Limitations to standard Parshall flume calibrations." *Proc., Nat. Conf. on Hydr. Engrg.*, San Diego, Calif., 915-920.

APPENDICES



Appendix A: Laboratory Photographs

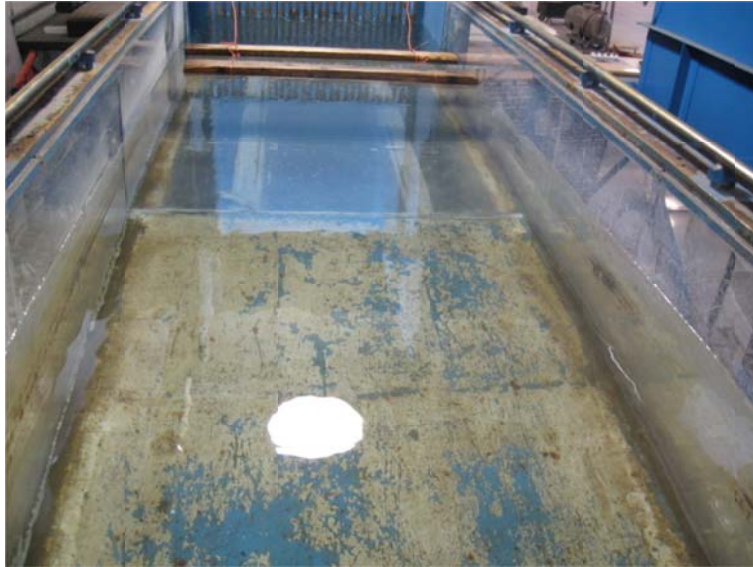


Figure 12. Upstream subcritical conditions. At a flow rate of 2.00 cfs, there are no surface waves, and the flow is subcritical. The flow direction is from top to bottom.



Figure 13. Hydraulic jump in the throat. At a flow rate of 1.50 cfs and submergence at 87%, the water is flowing from the canal back into the throat. The main flow direction is from left to right with the hydraulic jump moving against the main flow.

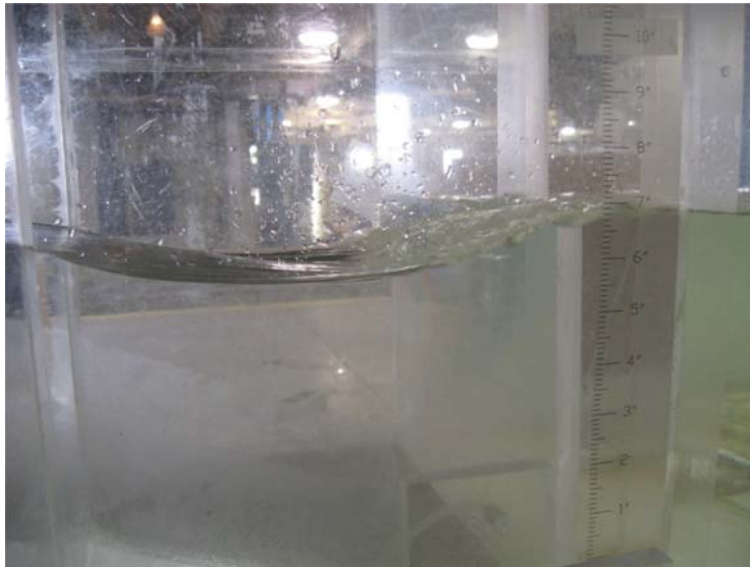


Figure 14. Initial unstable flow. At a flow rate of 0.50 cfs and submergence at 84%, the flow conditions are unstable. Picture 1 of 2 with water flowing left to right.



Figure 15. Secondary unstable flow. At a flow rate of 0.50 cfs and submergence at 84%, the flow conditions are unstable. Picture 2 of 2 with water flowing left to right. The two pictures are taken 5 seconds apart and demonstrate unstable hydraulic conditions experienced during laboratory testing.

Appendix B: Images from *Flow 3D*<sup>TM</sup>

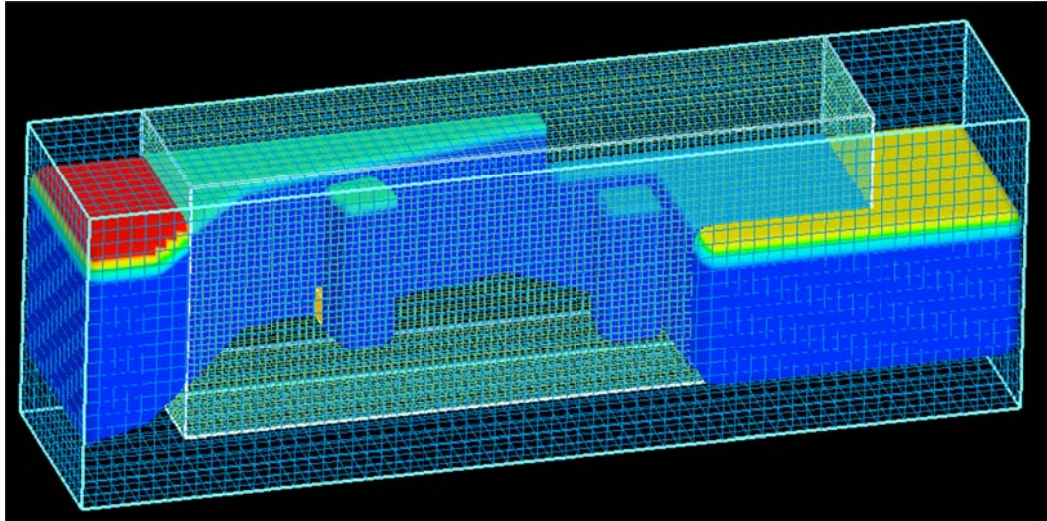


Figure 16. Initial water surface. At a flow rate of 2.00 cfs and submergence at 70%, the initial water surface conditions help minimize simulation time. The water flows from left to right, and the Montana flume is transparent.

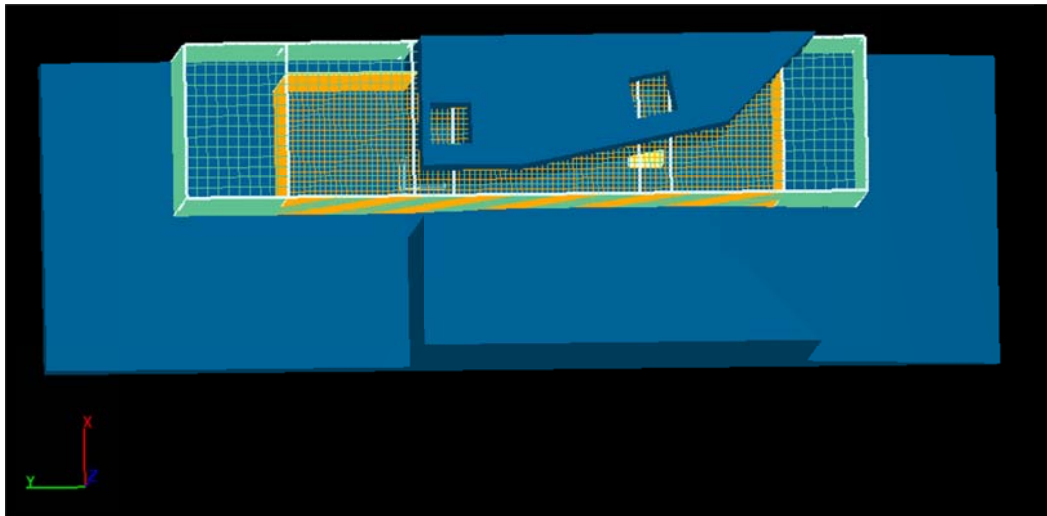


Figure 17. Flume meshing and geometry. The water would flow from right to left in this top view of the Montana flume geometry and meshing.

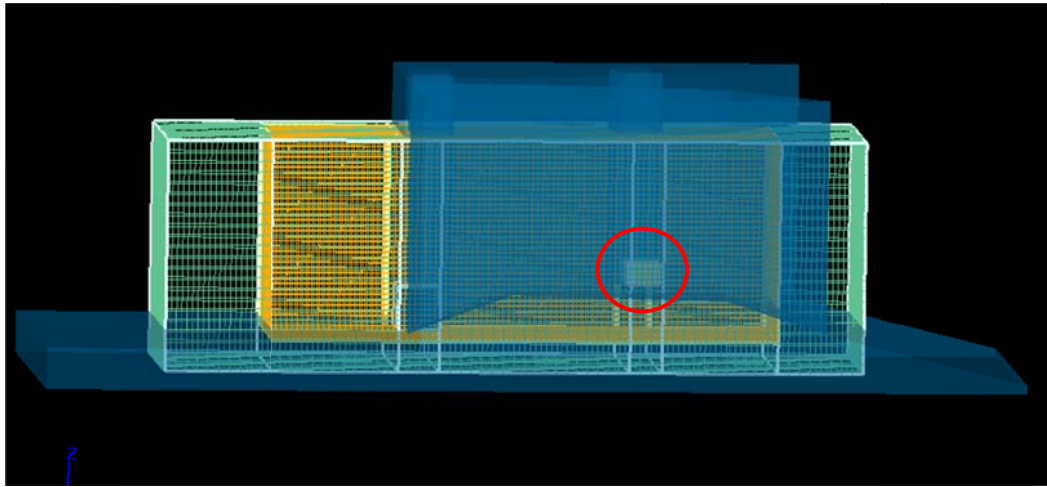


Figure 18. Refined mesh for stilling well. The refined mesh for the stilling well is circled, and the flume is semi-transparent. In this side view, water flows from right to left.

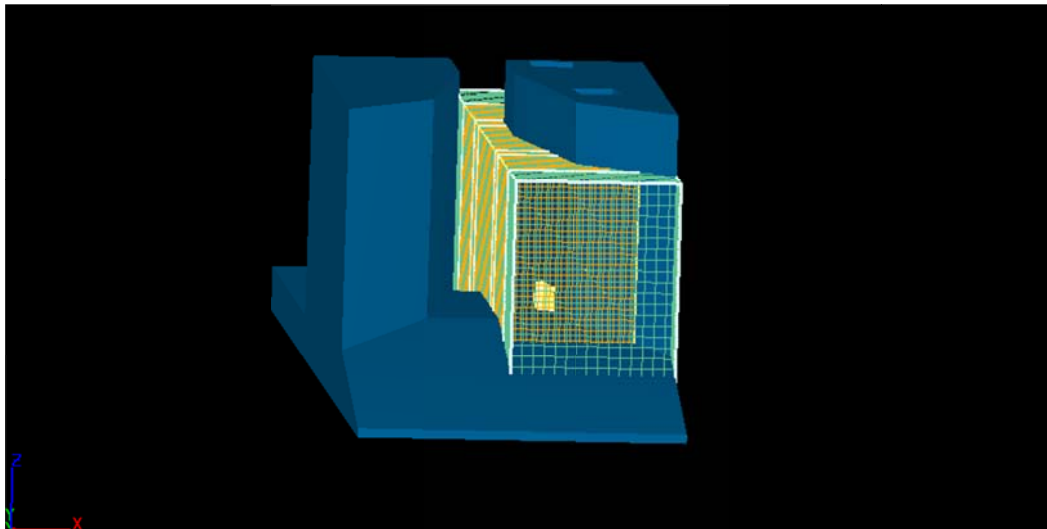


Figure 19. Upstream geometry and mesh. The Geometry and Mesh are shown as the water approaches the flume. The mesh doesn't start until wingwalls on the upstream side, and a nested mesh begins for the converging section.



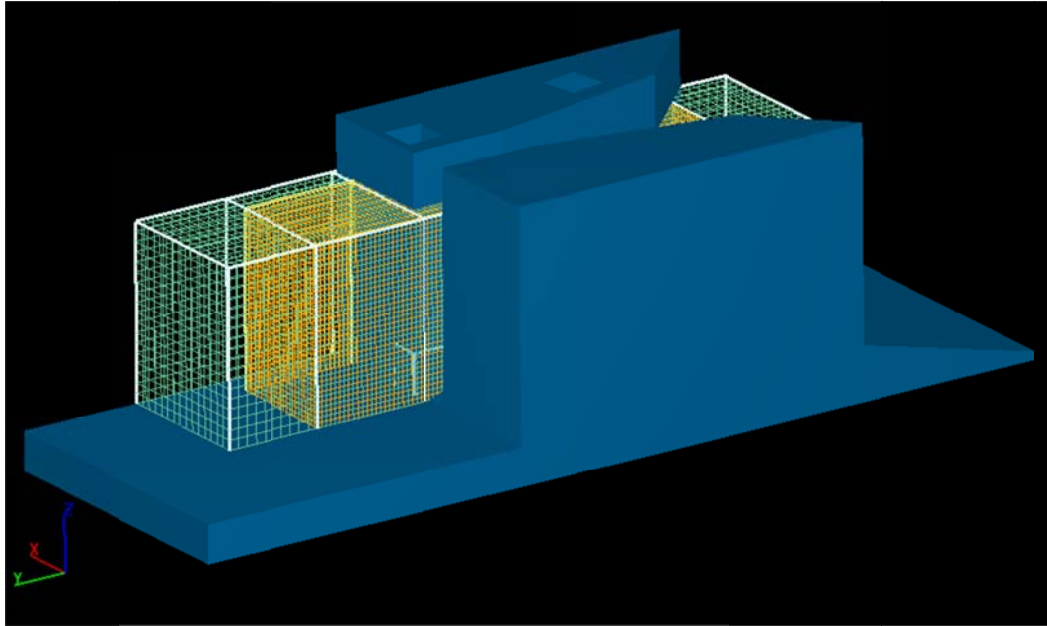


Figure 20. Downstream geometry and mesh. The Geometry and Mesh are shown as the water exits the throat of the flume. A more refined mesh needed to be used to properly simulate the turbulence downstream of the throat.

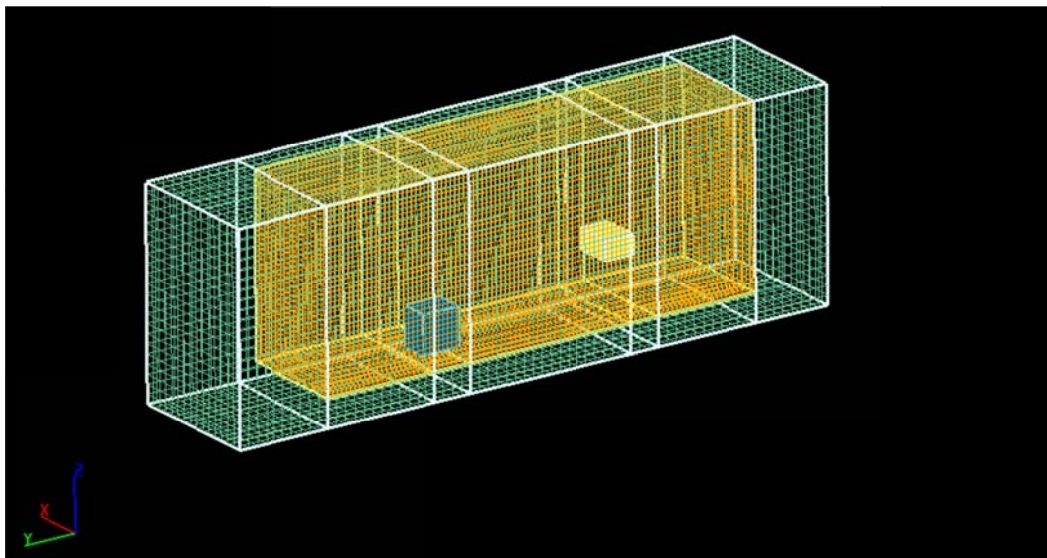


Figure 21. Nested mesh sizing. The largest grid represents a mesh where each cell size is 0.1 ft. The next smallest mesh contains cells of 0.05ft. The two smallest blocks are a refined meshes for the stilling well ports. These smallest mesh cells are 0.01 ft. The white lines represent fixed points along the length of the flume to aid in transferring information between nested meshes.